Effect of vacancy-type oxygen deficiency on electronic structure in amorphous alumina

Hiroyoshi Momida,[1,a)] Seisuke Nigo,[2] Giyuu Kido,[2] and Takahisa Ohno[1,2]
[1]*Institute of Industrial Science, University of Tokyo, 4-6-1 Komaba, Meguro, Tokyo 153-8505, Japan*
[2]*National Institute for Materials Science, 1-2-1 Sengen, Tsukuba, Ibaraki 305-0047, Japan*

(Received 1 October 2010; accepted 6 January 2011; published online 24 January 2011)

Electronic and atomic structures associated with a vacancy-type oxygen deficiency in an amorphous alumina model are studied by first-principles calculations. The energy levels of the oxygen defects significantly shift depending on their charge states because of remarkable changes of local atomic structures. That is different in character from the α crystal case. We discuss a possibility of the oxygen defects as a conductive path and present an atomistic mechanism of the resistive switching effects in the memory devices. © *2011 American Institute of Physics*. [doi:10.1063/1.3548549]

Alumina is a useful material for electronic device applications,[1,2] and amorphous phases are used in many of its applications rather than crystalline phases. Such applications require knowledge of defect levels in a band gap. However, the understanding of defect properties in the amorphous phases is limited compared with that in the crystalline phases. Comparative studies of amorphous and crystalline defects provide us with insight to clarify which is suitable for electronic device applications.

This work is motivated by the amorphous alumina as a candidate material for the resistive random access memory (ReRAM), which attracts great interest as a future nonvolatile memory.[3–6] The ReRAM has a capacitorlike structure and utilizes a reversible resistive switching effect operated by an applied voltage. Though the microscopic mechanisms of resistive switching are not yet clear, defects have been considered as a key factor for revealing its atomistic origin.[7–10]

For the amorphous alumina ReRAM, experimental analyses have shown the reduced O/Al ratio at the current conduction paths, and the electronic defect bands in the band gap have been observed.[3,4] The results suggest oxygen deficiencies as a possible cause of the current conduction paths. In this study, we perform first-principles calculations of the amorphous alumina with vacancy-type oxygen defects and discuss a ReRAM mechanism.

We used an amorphous Al_2O_3 periodic supercell model, which is composed of 48 Al and 72 O atoms/cell connected by the Al–O bonds.[11] The coordination numbers of Al in the model are four (60.4% of Al), five (29.2%), and six (10.4%), and the density is 3.27 g/cm^3, consistent with experimental results.[11–13] To study the vacancy-type oxygen deficiencies, a single O^{-q} ion (q=0, 1, or 2) was removed from the model structure and then the atomic structures were fully relaxed. This procedure was done for the 72 inequivalent O sites for each q (We describe the removed O^{-q} site as the vacancy V_O^q for both the α crystal and the amorphous model).

The first-principles calculations are based on the density functional theory (DFT) within the local density approximation (LDA) and the plane-wave pseudo-potential method,[14–17] and done by the PHASE code in nonmagnetic states. Charged defects were calculated by assuming the presence of a compensating uniform background.[18] A plane-wave cutoff energy of 25 Ry was used and self-consistency was attained by adopting the Γ only $\boldsymbol{k}$-point sampling. Atomic structures were relaxed until all atomic forces became less than 1 mRy/Bohr. To calculate the density of states (DOS), the $\boldsymbol{k}$-point sampling was increased to the uniform $4\times4\times4$ mesh.

The calculated band gap of the defect-free α-crystal 120-atom supercell is 6.04 eV, and that of the amorphous model is 3.76 eV. The experimental band gaps of the α and the amorphous phases are 8.8 and 5–7 eV, respectively.[11,19,20] The band gap of the amorphous is smaller than that of the α crystal in both the calculations and the experiments. Note, however, that the DFT-LDA calculations underestimate the experimental band gaps.

Figure 1 shows the DOS of the α crystal supercell with a single V_O^q. In the band gap, the energy levels associated with V_O^0 (fully-occupied state), V_O^{+1} (half-filled state), and V_O^{+2} (empty state) appear at 2.57, 3.07, and 3.66 eV relative to the bulk valence band edges, respectively. The level shift by q results from atomic structure relaxations at V_O. The Al–O bond lengths in the α crystal are 1.86 and 1.96 Å, and the Al-V_O distances are 1.81 and 1.98 Å (V_O^0), 2.00 and 2.07 Å (V_O^{+1}), and 2.17 and 2.15 Å (V_O^{+2}).

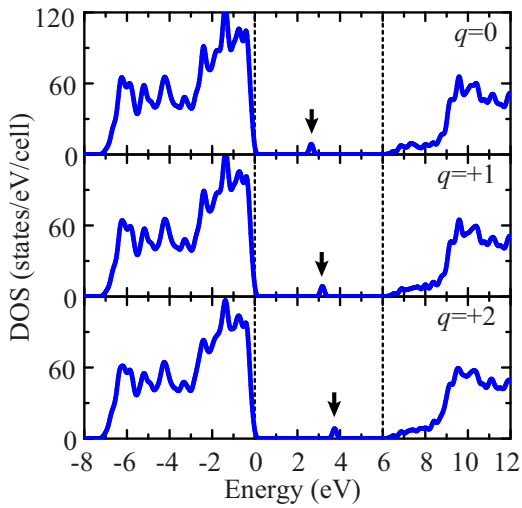

FIG. 1. (Color online) Calculated density of states (DOS) for the V_O^q in α crystal. Broken lines show bulk band edges. Arrows indicate mid-gap levels.

a)Electronic mail: MOMIDA.Hiroyoshi@nims.go.jp.

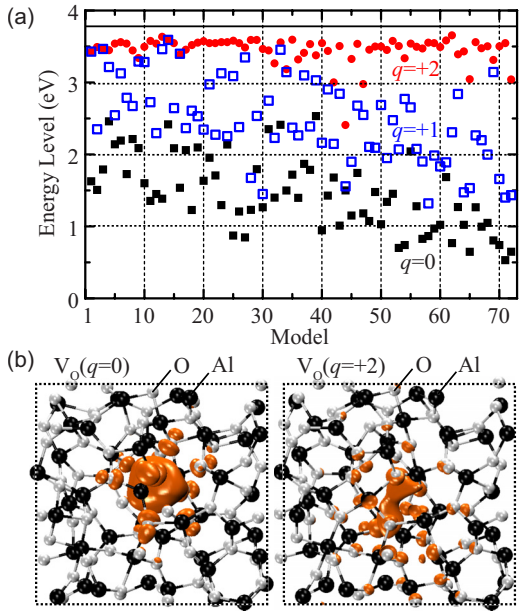

FIG. 2. (Color online) (a) Calculated mid-gap energy levels at the Γ of the V_O^qs in the amorphous model for $q=0$ (solid squares), +1 (open squares), and +2 (circles). Bulk band edges are at the energy origin and shown by the solid line. The model index of V_O is arranged in ascending order of its formation energy averaged over q, i.e., Model-1 is energetically most stable. (b) Model-1 structure for $q=0$ (left) and +2 (right). V_O is placed at the center of the unit cell. An isodensity surface of electron density of the mid-gap level is plotted for 0.002 e/Bohr^3.

Figure 2(a) shows the calculated energy levels of V_O^q in the band gap for the amorphous model. The energy levels appear in the band gap for all V_O^qs, and are scattered in a wide energy range depending on the removed O sites. The energy ranges are 0.51–2.51 eV (V_O^0), 1.30–3.58 eV (V_O^{+1}), and 2.39–3.64 eV (V_O^{+2}) relative to the bulk valence band edge. The levels shift higher in energy with increasing q for each individual V_O site. The statistical simple averages (standard deviations) of the energy levels are 1.44 eV (0.51 eV) (V_O^0), 2.47 eV (0.59 eV) (V_O^{+1}), and 3.43 eV (0.19 eV) (V_O^{+2}) relative to the bulk valence band edge. The averaged energy difference between V_O^q and V_O^{q+1} is about 1 eV, which is about twice as large as that in the α crystal. It is remarkable that the V_O^{+2} levels are in the narrow energy range and close to the bulk conduction band edge.

Figure 2(b) shows the partial electron density of the V_O^q level (the energetically most stable V_O). The V_O^0 level shows the spatially localized character and arises from the strong interaction between the neighboring Al orbitals with the small p-type orbitals of the surrounding O atoms. Compared with V_O^0, the unoccupied V_O^{+2} level shows the delocalized character with the high density at V_O. Similar delocalized V_O^{+2} characters in an amorphous HfO_2 have been also found by first-principles.[21]

Focusing attention on the energetically stable V_Os, there are many V_O sites where the energy difference between V_O^{+1} and V_O^{+2} is very small. This special character differs from the crystal case and the averaged character. Because such V_Os are relatively energetically stable, it is expected that these V_Os exist with a high frequency in amorphous phases.

Figure 3 shows the DOS for energetically stable V_O^qs. For the most stable V_O [Fig. 3(a)], the energy levels at the Γ are 1.61 eV (V_O^0), 3.41 eV (V_O^{+1}), and 3.41 eV (V_O^{+2}), which

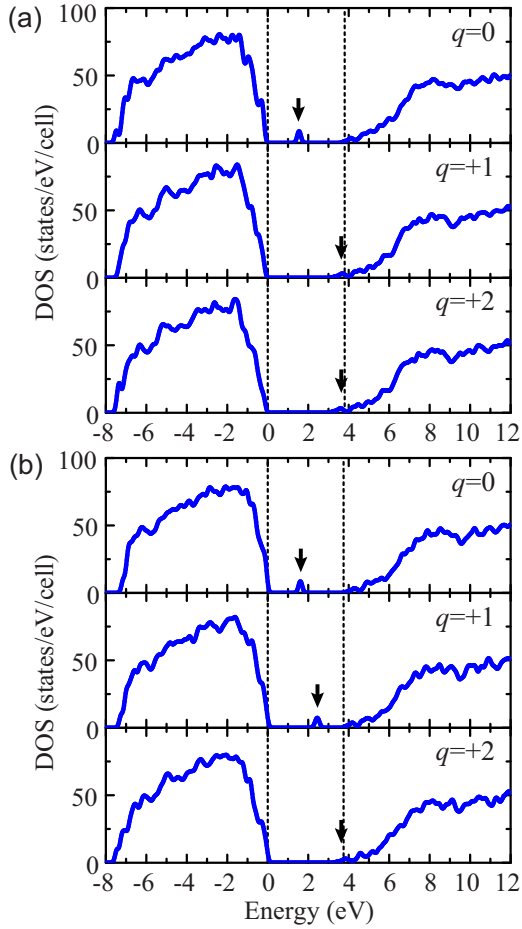

FIG. 3. (Color online) Calculated density of states (DOS) for the V_O^q in the amorphous model, (a) the most and (b) the second-most energetically stable V_Os. Broken lines show bulk band edges. Arrows indicate mid-gap levels.

shows the special character of the amorphous phase. For the second-most stable V_O [Fig. 3(b)], the levels are 1.49 eV (V_O^0), 2.33 eV (V_O^{+1}), and 3.47 eV (V_O^{+2}), and this shows the averaged character.

Figure 4 shows the atomic structures at the most and the second-most stable V_O^qs. After a neutral O atom is removed from the defect-free model, most of the Al neighboring the V_O move toward the V_O because of the interaction between

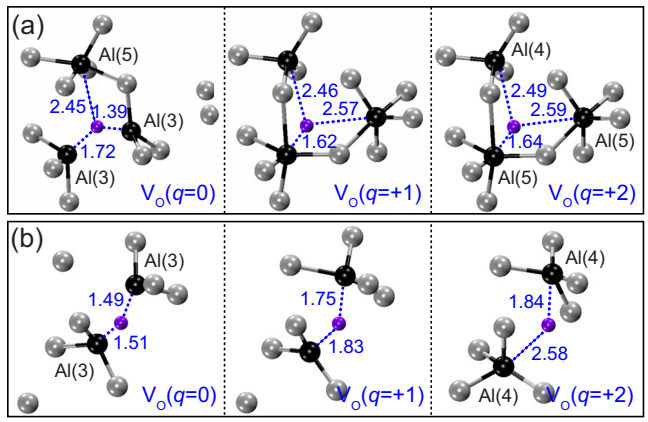

FIG. 4. (Color online) Local atomic structures of (a) the most and (b) the second-most energetically stable V_Os in the amorphous model. Al-V_O distances are in angstroms. O-coordination numbers of Al are shown in parentheses.

the neighboring Al, as shown in Fig. 2(b). Thus, for V_O^0, most of the Al-V_O distances are shorter than the corresponding Al–O distances in the defect-free model, and consequently, the Al–Al distances are shortened. The shortest Al–Al distance at V_O^0 (2.60 Å in the most stable model and 2.61 Å in the second-most stable model) is shorter than that in the α crystal (2.68 Å) and the nearest Al–Al distance in the fcc Al metal (2.86 Å).

Comparing V_O^{+2} with V_O^0, the local structure relaxation is significantly large and causes the coordination number changes of Al. The outward relaxations of Al and the inward relaxations of O from V_O are found in most cases due to the lack of interaction between the Al orbitals in the empty V_O^{+2} state and the ionic potential change. The changes of the Al-V_O distances by q in the amorphous are much larger than that in the α crystal, and this accounts for the larger energy level shift by q. The V_O^{+2} local structure is not apparently recognized as a vacancy unlike the crystal case, because the bulklike O-coordination of Al is recovered. This explains the reduced V_O character in Fig. 2(b) and the narrow width of the V_O^{+2} energy levels.

V_O^{+1} structures cause two types of energy level shifts by q (Fig. 3). In the most stable V_O [Fig. 4(a)], the V_O^{+1} structure is largely relaxed from the V_O^0 structure, and the atomic structures show very little change between V_O^{+1} and V_O^{+2}. Thus, this explains the little change of the energy levels between V_O^{+1} and V_O^{+2} [Fig. 3(a)]. In the second-most stable V_O [Fig. 4(b)], the Al-V_O distances gradually increase as the q increases. Thus, the V_O^q energy level increases gradually as the q increases [Fig. 3(b)].

The calculated results show that the V_O levels appear in the band gap. The formation of defect bands in the band gap can be speculated on if the V_O density becomes high enough to interact with each other. Thus, the V_O is a possible origin of the current conduction paths in the ReRAM, in addition to metallic Al defects pointed out experimentally.[5,6]

Finally, we propose an atomistic mechanism of the resistive switching assuming high a V_O density. When V_Os are in filled states by electron injection, Al atoms become close and then a metallic band appears in the band gap. When V_Os are in empty states by electron ejection, Al atoms move away from the V_O with large energy level shifts toward the bulk conduction band edge (i.e., the vacancy character is suppressed); thus, disconnections of the mid-gap electronic conduction paths occur. Former and later correspond to low and high resistance states, respectively. The V_O formation/annihilation by O migrations reported previously for transition-metal oxides[8,10] is also a candidate mechanism in amorphous alumina. If the presented mechanism is the dominant cause of the resistive switching, an amorphous seems to be more suitable for a ReRAM material than crystals, because the energy levels and atomic structures associated with V_O are more sensitive to its charge states.

A part of this work was supported by the RISS Project of the IT program and the Elements Science and Technology Project of the MEXT, Japan.

[1]G. D. Wilk, R. M. Wallace, and J. M. Anthony, J. Appl. Phys. **89**, 5243 (2001).
[2]J. A. Kittl, K. Opsomer, M. Popovici, N. Menou, B. Kaczer, X. P. Wang, C. Adelmann, M. A. Pawlak, K. Tomida, A. Rothschild, B. Govoreanu, R. Degraeve, M. Schaekers, M. Zahid, A. Delabie, J. Meersschaut, W. Polspoel, S. Clima, G. Pourtois, W. Knaepen, C. Detavernier, V. V. Afanas'ev, T. Blomberg, D. Pierreux, J. Swerts, P. Fischer, J. W. Maes, D. Manger, W. Vandervorst, T. Conard, A. Franquet, P. Favia, H. Bender, B. Brijs, S. Van Elshocht, M. Jurczak, J. Van Houdt, and D. J. Wouters, Microelectron. Eng. **86**, 1789 (2009).
[3]S. Kato, S. Nigo, J. W. Lee, M. Mihalik, H. Kitazawa, and G. Kido, J. Phys.: Conf. Ser. **109**, 012017 (2008).
[4]J. Lee, S. Nigo, Y. Nakano, S. Kato, H. Kitazawa, and G. Kido, Sci. Technol. Adv. Mater. **11**, 025002 (2010).
[5]S. Kim and Y.-K. Choi, Appl. Phys. Lett. **92**, 223508 (2008).
[6]W. Zhu, T. P. Chen, Z. Liu, M. Yang, Y. Liu, and S. Fung, J. Appl. Phys. **106**, 093706 (2009).
[7]G. Dearnaley, A. M. Stoneham, and D. V. Morgan, Rep. Prog. Phys. **33**, 1129 (1970).
[8]M. Fujimoto, H. Koyama, M. Konagai, Y. Hosoi, K. Ishihara, S. Ohnishi, and N. Awaya, Appl. Phys. Lett. **89**, 223509 (2006).
[9]R. Waser and M. Aono, Nature Mater. **6**, 833 (2007).
[10]A. Sawa, Mater. Today **11**, 28 (2008).
[11]H. Momida, T. Hamada, Y. Takagi, T. Yamamoto, T. Uda, and T. Ohno, Phys. Rev. B **73**, 054108 (2006); **75**, 195105 (2007), and references therein.
[12]T. Iijima, S. Kato, R. Ikeda, S. Ohki, G. Kido, M. Tansho, and T. Shimizu, Chem. Lett. **34**, 1286 (2005).
[13]S. K. Lee, S. B. Lee, S. Y. Park, Y. S. Yi, and C. W. Ahn, Phys. Rev. Lett. **103**, 095501 (2009).
[14]P. Hohenberg and W. Kohn, Phys. Rev. **136**, B864 (1964).
[15]W. Kohn and L. J. Sham, Phys. Rev. **140**, A1133 (1965).
[16]J. P. Perdew and Y. Wang, Phys. Rev. B **45**, 13244 (1992).
[17]D. Vanderbilt, Phys. Rev. B **41**, 7892 (1990).
[18]C. G. Van de Walle and J. Neugebauer, J. Appl. Phys. **95**, 3851 (2004), and references therein.
[19]R. H. French, J. Am. Ceram. Soc. **73**, 477 (1990).
[20]S. Miyazaki, J. Vac. Sci. Technol. B **19**, 2212 (2001).
[21]P. Broqvist and A. Pasquarello, Microelectron. Eng. **84**, 2022 (2007).